

Running title: INTERTIDAL BAR EVOLUTION ON A HIGH-ENERGY BEACH SYSTEM**Title:** FIELD MEASUREMENTS OF INTERTIDAL BAR EVOLUTION ON A HIGH-ENERGY BEACH SYSTEM**Authors:** D.W.T. JACKSON¹, J. A. G. COOPER^{1,4}, M. O'CONNOR¹, E. GUISADO-PINTADO^{1,2}, C. LOUREIRO^{1,3,4}, G. ANFUSO⁵

¹Centre for Coastal and Marine Research, School of Environmental Sciences, University of Ulster, Cromore Road, Co. Londonderry, BT52 1SA, Northern Ireland.

²Coastal Environments Research Group, University Pablo de Olavide, Ctra. Utrera Km1 41013, Sevilla, Spain,

³Centro de Investigação Marinha e Ambiental, Universidade do Algarve, Campus de Gambelas, 8005-139 Faro, Portugal,

⁴School of Agriculture, Earth and Environmental Sciences, University of KwaZulu-Natal, Private Bag X54001, Durban, South Africa

⁵Department of Earth Sciences, School of Environmental and Marine Sciences, University of Cadiz, Puerto Real, Cadiz, Spain

¹Corresponding author, Email: d.jackson@ulster.ac.uk.

Keywords: bars, slip faces, beach**ABSTRACT**

Nearshore bars play a pivotal role in coastal behaviour, helping to protect and restore beach systems particularly in post-storm conditions. Examination of bar behaviour under various forcing conditions is important to help understand the short to medium term evolution of sandy beach systems. This study carried out over a nine-week period examines, the behaviour of three intertidal bars along a high energy sandy beach system in northwest Ireland using high-frequency topographic surveys and detailed nearshore hydrodynamic modelling.

Results show that, in general, there was onshore migration for all the bars during the study period, despite the variability observed between bars, which was driven mostly by wave dominated processes. Under the prevailing conditions migration rates of up to 1.83 m day⁻¹ and as low as 0.07 m day⁻¹ were observed. During higher wave energy events the migration rates of the bars decelerated in their onshore route, however, under lower wave energy conditions, they quickly accelerated maintaining their shoreward migration direction. Tidal influence appears to be subordinate in these conditions, being restricted

to moderating the localised wave energy at low tides and in maintaining runnel configurations providing accommodation space for advancing slip faces.

The study highlights the intricate behavioural patterns of intertidal bar behaviour along a high energy sandy coastline and provides new insights into the relative importance of wave and tidal forcing on bar behaviour over a relatively short time period.

1. INTRODUCTION

1 Sand bars are common features of sandy beach systems in both intertidal (Ruessink and
2 Terwindt 2000; Ruessink et al., 2002) and subtidal (Gelfenbaum and Brooks 2003)
3 domains and in microtidal (Roy et al., 1994) to macrotidal (Levoy et al., 2000) regimes.
4 They occur in swell-dominated to storm-wave conditions with changes in bar location
5 and amplitude influencing beach and dune sediment supply regimes. Two reviews
6 (Wijnberg and Kroon 2002; Masselink et al., 2006) have presented classification schemes
7 for intertidal bars and three main types have been identified on the basis of morphology
8 and environmental setting *viz.* *slip-face bars*, *low amplitude ridges* and *sand waves*. *Slip-*
9 *face bars* have been described as having relatively large morphological amplitude; *low-*
10 *amplitude ridges* are expressed as subdued topography whilst *sand waves* are labelled as
11 ‘marginal repetitive features’. Slip-face bars display a distinctively steep, landward-
12 facing slip-face (slope usually $>30^\circ$) and low angle seaward slope ($<3-6^\circ$), with crest to
13 trough heights generally over 1m. Low-amplitude ridges usually position themselves
14 shore-parallel and group themselves into two to six bars, similar to what has been
15 described as ridge and runnel topography. Crest to trough height does not normally
16 exceed 1m in elevation and bar spacing is around 100m. The seaward slope of low-
17 amplitude ridges is around $2-4^\circ$ and we usually find them located within the entire
18 intertidal profile. Flat, low to medium energy beaches, with meso- or macro-tidal ranges
19 are typical settings of this bar type. Intertidal sand waves are defined as straight or
20 slightly sinuous, shore parallel and similar in morphology to sub-tidal sand waves. These
21 features are the most morphologically subdued bar forms but can number from around
22 four up to twenty. Rarely exceeding 0.5m in height their spacing is around 50m with a
23
24

25 symmetric cross-section and slopes of 1-3°. A common setting for this bar type is low
26 energy, low inter-tidal slope but can occupy a range of tidal range environments
27 (Masselink et al., 2006).

28

29 Formation of bars is normally associated with storm activity whereby material is eroded
30 from beach/dune systems by wave action and moved offshore. Sediment reworking
31 onshore during the post-storm phase typically involves initial formation of a ridge(s) over
32 several tidal cycles. Once the ridge is formed, and providing wave energy is low to
33 moderate, the bar stabilises or migrates onshore across the intertidal zone (Aagard et al.,
34 2006). Bar migration occurs as long as swash action can overtop the bar crest; the ridge
35 crest may stabilise when tides change from springs to neaps and overtopping ceases
36 (Masselink et al., 2006). Under the latter conditions swash and backwash still operate on
37 the seaward slope and an overall increase in elevation of the feature occurs due to
38 accretion on the seaward edge. The bar-face may then be trimmed by currents flowing in
39 the troughs (Anthony et al., 2005).

40

41 Circulation patterns and wave activity in the nearshore are directly influenced by the
42 presence of bars, which in turn, dictate the patterns of sediment transport within the surf
43 and swash zones (Jackson et al., 2007). Local tidal variability and wave climate
44 determine the extent to which hydrodynamic conditions alter and shape nearshore bars
45 (Wijnberg and Kroon 2002; Gelfenbaum and Brooks 2003). Traditionally, the concept of
46 *onshore* movement of sand bars has been associated with fair-weather conditions in the
47 aftermath of winter storms that caused initial *offshore* movement of sand (Aubrey 1979;

48 Thornton et al., 1996; Gallagher et al., 1998). However, the number of accounts of the
49 mechanisms and patterns of *onshore* sediment movement in bars are surprisingly few and
50 direct field quantification of bar movement is rare (Elgar et al., 2001; Aagard et al.,
51 2006). Both laboratory and field studies have, however, proposed that fluid accelerations
52 and velocities are largely responsible for driving sediment transport and, subsequently,
53 sand bar migration across the surf zone (Osborne and Greenwood 1993; Jaffe and Rubin
54 1996).

55

56 Recorded migration rates of intertidal bars vary considerably from virtually static to
57 values of around 1 m day^{-1} in low to moderate wave energy conditions (Wijnberg and
58 Kroon 2002). Rates of up to 5 m day^{-1} have been noted in higher wave energy regimes
59 (Elgar et al., 2001; Aagard et al., 2006). As bars migrate landward they become subject to
60 less frequent overtopping and may ultimately weld to the shoreline as the intervening
61 runnel is in-filled (Aagard et al., 2006). Anthony et al (2004; 2005) suggested that the
62 presence of strong trough (runnel) flows can be an important control on bar migration and
63 Aagard et al. (2006) demonstrated that the infilling of the trough can affect bed return
64 flows, also a key determinant in the dynamics of bar migration.

65

66 Several authors have identified diurnal tidal variation as a major control on bar
67 behaviour. Wijnberg and Kroon (2002) contend that bars migrate more rapidly under
68 spring tidal conditions when overtopping is more frequent. In contrast Masselink et al.
69 (2006) suggest that neap tides produce vertical focussing of wave action within a narrow
70 band and hence bars are more active under those conditions. Wijnberg and Kroon,

71 (2002) considered that high-energy waves cause an increase in set-up and consequently
72 undertow may temporarily become dominant over the intertidal beach, resulting in bar
73 destruction and flattening of the beach.

74

75

76 The beach and dunes at Five Finger Strand (Northwest Ireland) are adjacent to a tidal
77 inlet and associated ebb-tide delta. Analysis of historical patterns of behaviour of the
78 system (Cooper et al., 2007) indicates that periodic switches in position of the ebb
79 channel at a multi-decadal timescale are the main driver of long-term coastal behaviour.
80 During each of these channel switches, a new ebb delta forms at the channel terminus,
81 drawing in sand from the adjacent beach. This causes the beach to be lowered and
82 enables waves to penetrate to the vegetated dunes and erode them. The records in this
83 study relate to the early stages of this reworking under conditions of abundant sediment
84 supply and available depositional space (accommodation space) on the adjacent beach.
85 Such conditions are rare and offer an unusual insight into bar migration.

86

87 This paper outlines field measurements of intertidal bar evolution on a high-energy beach
88 system. The nature of the bars is described and their behaviour and morphological
89 evolution over a 9-week period is outlined in the context of direct forcing variables
90 (waves and tides). These observations provide an opportunity to test the existing models
91 of intertidal bar behaviour presented by Wijnberg and Kroon, (2002) and Masselink et al.
92 (2006) and in particular to assess the comparative role of wave conditions and tidal
93 variation.

94

95

2. STUDY AREA

96

97 Five Finger Strand is situated on the north coast of the Inishowen Peninsula, Co.
98 Donegal, Ireland. The beach extends for approximately 1.7km in a north-south direction
99 between the Five Fingers Rock and Lagg Point at the narrow inlet of Trawbreaga Bay
100 (Fig.1). The strand maintains a modally dissipative beach (Wright and Short, 1984)
101 whose intertidal zone is 350m wide, backed by a large vegetated dune system. The beach
102 sediment comprises carbonate-rich terrigenous sand (mean grain size 0.21 mm and
103 largely homogenous) with a subordinate gravel component overlying a cobble/gravel
104 base of glacial sediments. The mean spring tidal range at the site is 3.3 m. The open
105 coast is swell wave dominated with a modal significant wave height of ca. 2.2m and
106 period 9s. The dominant swell approach is from the W and SW and waves are fully
107 refracted within the headland-embayment system (Jackson et al., 2005).

108

INSERT FIG. 1

109

110 The mesoscale (decadal) dynamics of the site is driven by tidal inlet switching and tidal
111 delta formation and abandonment in that when the ebb channel switches, the former
112 channel is abandoned and the sediment stored in its delta is then reworked by wave action
113 (Cooper et al., 2007; O'Connor et al., 2011). The observations reported in this paper were
114 made during a phase of ebb delta reworking through the formation and dominantly
115 landward migration of a set of subtidal and intertidal bars (Fig. 1). The beach lowering
116 associated with initial channel migration produces a large accommodation (depositional)

117 space for later sediment accumulation and the sand being reworked from the ebb delta
118 provides an abundant sediment supply.

119

120

3. METHODOLOGY

121

122 Profile information was gathered using DGPS along a number of fixed profile lines
123 established on the 1.7 km stretch of beach between 1st July and 10th September 2003. A
124 quad bike-mounted DGPS surveying system (Trimble 4400) was employed to acquire
125 topographic information. The typical precision of an initialised kinematic survey is 10
126 mm + 2ppm (1 standard deviation) (Huang et al., 2002). Surveys were reduced to the
127 national datum (Irish Ordnance Datum (OD) Poolbeg, Dublin).

128 Repeat topographic surveys at fixed positions enabled the chronological changes in bar
129 morphology to be established over the 9-week period. From these data the rates of slip
130 face movement and crest height evolution were extracted. In order to characterise the
131 intertidal bars and their behaviour, two profiles (profile lines 1 and 3, Fig. 2) were
132 selected for analysis, as they consistently pass through the main body of the bars and are
133 representative of the entire beach. Profile 1 intersects Bars A and C and Profile 3 passes
134 through Bar B.

135

INSERT FIG. 2

136

137 Offshore wave data were recorded by the Marine Institute M4 wave buoy (inset in Fig.
138 1), located in approximately 56 m water depth in the northwestern Irish shelf (54° 24', N
139 9° 02'W) from which deep-water wave conditions (hourly significant wave height and

140 mean wave period) for the duration of the survey period were obtained. Given the
141 absence of directional measurements, wave direction was obtained from the hindcast Met
142 Office UK Waters Wave Model (Golding 1983; Bradbury et al., 2004) for a grid cell
143 coincident with the M4 buoy location, as this model presents a very good agreement with
144 the buoy records for the study period ($R = 0.85$ and $RMSE = 0.37$ for significant wave
145 height). The hindcast model wave direction data is provided on a 3-hour interval and was
146 linearly interpolated to match the hourly frequency of the wave buoy data.

147 The offshore wave conditions (H_s – significant wave height, T_m – mean wave period; Dir
148 – mean wave direction) were used to force the nearshore propagation with SWAN wave
149 model (Booij et al., 1009, Ris et al., 1999). SWAN was implemented using a nested
150 modelling scheme, with modelling domains composed of a 30m resolution local grid
151 around the Five Finger Strand area, nested into a regional 100m resolution grid extending
152 from the M4 location to the Inishowen Peninsula area (Fig. 3). Simulations were run at
153 hourly intervals from the 1st of July to the 20th of September 2003 with the parametric
154 data from the buoy and hindcast model applied uniformly to the offshore boundary,
155 considering a JONSWAP spectral shape to represent the wave field and variable water
156 levels. SWAN was run in third-generation mode, using default parameters for linear wave
157 growth and whitecapping dissipation, JONSWAP bottom friction dissipation model
158 following Hasselmann et al. (1973), and depth-induced breaking imposed by a scaled
159 breaker index according to the β -kd model for surf-breaking (Salmon and Holthuijsen
160 2011). The wave frequency and directional space were discretized in 33 logarithmic-
161 distributed bins from 0.03 to 1.00 Hz and 36 regular distributed bins, respectively.

162 The two regular bathymetric grids used for the simulations, with 100m and 30m
163 resolutions, were compiled from high-resolution multibeam and airborne LIDAR data
164 collected in the framework of the Joint Irish Bathymetric Survey (JIBS) and the
165 Integrated Mapping for the Sustainable Development of Ireland's Marine Resource
166 (INFOMAR) project. The nearshore bathymetry of the Five Finger Strand embayment,
167 landward of 9m-depth contour, was obtained using a linear transform algorithm applied
168 to multispectral Landsat imagery tuned with multibeam and LIDAR data from a nearby
169 location, following the procedure described in Pacheco et al. (2015). Bathymetric data,
170 provided in LAT (Lowest Astronomical Tide) were reduced to mean sea level
171 (approximately +2.2m OD Poolbeg, Dublin).

172

173 **INSERT FIG. 3**

174

175 SWAN output variables computed included H_s , peak (T_p) and mean (T_m) wave period, as
176 well as mean (Dir) and peak ($DirP$) wave direction. These were extracted at hourly
177 intervals for a set of grid points located in the centre of the embayment and
178 approximately 5m below mean sea level (equivalent to -2.8m OD Poolbeg, Dublin).
179 Wave data for these locations was averaged, providing a time-series of nearshore waves
180 in the area of incipient wave breaking for the duration of the study period.
181 Water levels were obtained from the astronomical tide predictions for the local tidal
182 gauge (Malin Head). Records were subsequently reduced to OD Poolbeg, Dublin, and
183 used to characterize water level variations and compute the daily maximum tidal range.

184 In order to relate intertidal bar geomorphic evolution with hydrodynamic forcing and
185 quantify the combined influence of waves and tides in bar migration rates, the normalised
186 wave power (Pn) was computed according to Morris *et al.* (2001):

$$187 \quad Pn = P(\eta_{\text{dtr}}/\eta_{\text{str}}) \quad (1)$$

188 where η_{dtr} is the maximum daily tidal range, η_{str} is the maximum spring tidal range, and P
189 is the wave power, given by:

$$190 \quad P = ECg \quad (2)$$

191 where E is the wave energy computed according to linear wave theory:

$$192 \quad E = (1/8)pgH_s^2 \quad (3)$$

193 and Cg is the wave group velocity, which according to the shallow water approximation
194 is obtained by:

$$195 \quad Cg = \sqrt{gh} \quad (4)$$

196 where p is the density of water and g is the acceleration due to gravity and h is the
197 nearshore water depth.

198 The Pn parameter has been shown to adequately reflect the enhanced erosion potential
199 during spring tides, restricting it for lower tidal ranges (Morris *et al.*, 2001) and applied to
200 investigate hydrodynamic forcing and morphological change in mesotidal beaches
201 (Loureiro *et al.*, 2012), as well as to force equilibrium models of 3D morphological
202 change (Stokes *et al.*, 2015).

203

204

205

4. RESULTS

206

207

4.1. Bar Morphology and Type

208

209 Figure 2 shows the plan and cross-sectional morphology of the intertidal beach and bars.
210 In plan form, the bars have discontinuous, sinuous crests with a shore-parallel orientation.
211 The overall intertidal beach slope (MHWN-MLWN positions) averages 0.69° in the south
212 where one intertidal bar is present and 0.25° in the north where there are two intertidal
213 bars. In cross-section (Fig. 2ii and iii) the bars are strongly asymmetrical. They have
214 gently sloping seaward faces with a consistent slope of around 0.7° and a steep landward
215 face that slopes between 3 and 15° into a landward runnel. The bars are typically around
216 1 m in height and 150m wide. This combination of features characterises them as
217 intertidal slip face bars (Masselink et al., 2006).

218

219 The position in the tidal frame of each bar differs. At the start of observations, the crest
220 of Bars C and B were located below the neap high tide level (ca 2.3 m and 2.7m.
221 respectively) and were therefore overtopped at every high tide. Bar A was located higher
222 in the tidal frame (ca 3.0 m) and was overtopped less frequently.

223

224

225 ***4.2. Intertidal Bar Geomorphic Evolution***

226

227 The geomorphic behaviour of the intertidal bars is described using topographic profiles
228 that contain two (Profile 1) or one (Profile 3) intertidal bars. Profile 1 on the northern
229 section of the beach shows the development of two bars (A and C) and associated
230 runnels. The net behaviour observed during the 9 weeks of observations was of slip face

231 landward migration by transport of sediment from the stoss side and eventual infilling of
232 the runnel (Fig. 4i). The elevation of the leading edge of the bars showed a general
233 increase as the bars migrated onshore across the intertidal beach. The elevation of the bar
234 crests rose over the study period. For bar C in particular, where it was initially located
235 below mean high water neap (and covered at every high tide), it was then positioned
236 above that level, when it was no longer covered by every tide. Detailed examination,
237 however, reveals differences in the evolution of the two runnel systems on this profile.
238 The seaward runnel that separates the two bars was infilled by rapid crest migration of
239 bar C. This was associated with gradual reduction in height of the slip face (Fig. 4iii) as
240 the runnel shallowed and was reduced in its cross-sectional area. Eventually, the rapidly
241 advancing slip face ridge of Bar C merged with the slowly migrating stoss side of Bar A.
242 At this stage, the intervening runnel was totally infilled, and the two former bars merged
243 to form a single entity.

244

245 The runnel landward of Bar A (Fig. 4ii) was initially deeper and was infilled by a slower
246 rate of slip face advance than that of Bar C because of a larger discharge in the runnel.
247 This migration caused a reduction in cross-sectional area of the runnel as it infilled by
248 slip face advance and therefore a loss of competence aiding in the process of infilling and
249 hence represented a positive feedback in the system.

250

251

252 During landward migration, the bars became slightly wider as the slip face advanced
253 more rapidly than the stoss face. This suggests that cannibalisation of the stoss side is

254 feeding the advance of the slip face and that the bar is eventually ‘smeared’ across the
255 beachface. Up to the point at which the two bars merged, however, they essentially
256 maintained their cross-sectional form as they migrated upwards and landwards. The slip
257 face remained at a consistent angle throughout the bar migration until the point just
258 before the bars welded.

259 **INSERT FIG.4**

260

261 Profile 3 (Fig.5) contained a single slip face ridge whose landward face migrated steadily
262 shoreward over the study period. Its seaward face, however, remained in essentially the
263 same position. The flat, upper surface of the bar extended landward without substantial
264 vertical accretion. Thus the bar became wider but maintained its vertical position. The
265 net effect was for landward infilling of the runnel as the bar extended in that direction.
266 The bar crest remained at and/or around neap high tide levels throughout the study.

267

268 **INSERT FIG.5**

269

270 In contrast to Bars A and C which maintained their form as they migrated, Bar B became
271 progressively wider. This situation is indicative of an offshore sediment supply that
272 enabled the crest to advance without the need for cannibalisation of the bar’s stoss slope.
273 Bar B is buffered by a more extensive sediment body between itself and the channel,
274 offering a ready sediment supply, as opposed to Bars A and C which were positioned
275 closer to the main channel and were fronted by a much reduced sediment body (supply)

276 width. In both cases, the slip face maintained a steep profile throughout its landward
277 migration and did not actually weld to the subaerial beach during the study period.

278

279

280

281

4.3. Bar Migration Rates

282 To compute bar migration rates, bar positions were measured during each survey that
283 took place with a time interval of 3 to 5 days. For calculation purposes, a constant rate of
284 movement was assumed throughout inter-survey periods. The rates were obtained by
285 comparing the total movement of each bar between surveys and then compared to the
286 average wave height (H_s) and normalised wave power (Pn) during those 3-5 days for
287 which the bars were migrating.

288 Figure 6 shows the migration rates for each of the bars based on the position of the mid-
289 slip face point in relation to the hydrodynamic forcing variables considered. Migration
290 rates, calculated by dividing the total displacement of mid-slip face by the number of
291 days between surveys, varied between offshore-directed 0.38 m day^{-1} and onshore-
292 directed 1.83 day^{-1} . The majority of movements were onshore-directed.

293

INSERT FIG.6

294

295 Mean wave forcing during the study period reveals a low to medium energy nearshore
296 environment with mean H_s of 0.81m, T_m around 6 s and waves approaching from WNW
297 (299°). Four relatively high-energy wave events ($H_s > 1.5\text{m}$) with W-WNW direction
298 occurred during 10th-12th July, 1st-3rd August 19th-23rd August and 6th-8th September ,

299 during which average nearshore significant wave heights were 1.78, 1.76, 1.35 and 1.5 ,
300 respectively (Fig.6ii). Maximum nearshore significant wave heights during these events
301 reached 2.13, 2.3, 1.85 and 2 m while averaged storm normalised wave power levels were
302 11075, 16495, 5349 and 11869 W/m, respectively. Each of these high-energy events was
303 accompanied by a deceleration (ascending sections of the lines in Fig. 6i) in subsequent
304 bar migration rates on Bar C and Bar A (Fig.6). Bar A, which is closest to the shore and
305 limited seaward by Bar C, showed less vigorous response to the variations in
306 hydrodynamic forcing. Bar B, which is relatively sheltered by offshore subtidal sediment
307 bodies and the tidal channel, displays slower onshore migration rate over the study
308 period.

309

310

INSERT FIG.7

311

312 Correlation analysis of migration rates with the normalised wave power (Fig.7) reveals
313 an apparent increase in bar migration rate with more energetic conditions and this is
314 mostly evident at Bar C (Fig. 7iii), while no statistical significant correlation is found for
315 Bar A and B. Furthermore, under more energetic forcing ($P_n > 6000 \text{ Wm}^{-1}$), no clear
316 correlation between bar migration and normalised wave power is apparent, possibly due
317 to increased water levels (positive surge) and hence less efficient wave-seabed
318 interaction. Other factors (e.g. position in the tidal frame, proximity to the tidal inlet etc.)
319 may therefore be assuming greater importance as wave height is reduced.

320

321 On Bar A, which is sheltered by Bar C, results suggest a possible tidal influence on
322 migration rates. During spring tides there is tendency for onshore migration rates to slow
323 (Fig. 6) compared to those of neap tides for similar wave energy levels. This suggests
324 that in those conditions, spring tides increase the flux of water through the runnel and
325 cause more erosion of the slip face than can be countered by wave-induced deposition.

326

327

5. DISCUSSION

328 The observations reported here can be compared with published observations of slip-face
329 bar behaviour in other settings. The typical conditions under which intertidal slip-face
330 bar formation and migration is reported relate to short-term storm recovery phases
331 (Wijnberg and Kroon 2002; Masselink et al. 2006) when storm-eroded sediment is
332 reworked under ensuing fair-weather conditions. The conditions reported here are similar,
333 in that they involve sediment reworking following erosion (associated with relatively
334 high wave energy events) but unusual because of the timescale under which the post-
335 erosion recovery period occurs. This prolonged period in a high-energy wave climate
336 setting increases the likelihood of occurrence of high wave conditions during the
337 recovery phase and thus could strongly affect onshore bar migration patterns.

338

339 The bar migration rates recorded in the study area range from below close to 0 m day^{-1} up
340 to almost 2 m day^{-1} , and thus similar to those recorded by Wijnberg and Kroon (2002)
341 who reported observations during low to moderate wave energy associated with 1 m day^{-1}
342 migration rates. Wave energy is a dominant factor in the behaviour of the more exposed
343 intertidal bars in the study area (especially bar C and to a lesser extent A), and appears to

344 be more important than variations in tidal range that have been reported elsewhere
345 (Wijnberg and Kroon 2002; Masselink et al., 2006).

346

347 The more sheltered Bar A does show a loose relationship between migration rate and
348 tidal range. These observations, however, contrast with those of Wijnberg and Kroon
349 (2002) who found that bars migrate onshore more rapidly during spring tides due to more
350 frequent overtopping. After welding of Bar C to Bar A there was an acceleration in the
351 onshore migration rate of the slip face of the newly merged bar. This may be attributed
352 to a new influx of sediment as the bars welded and/or a period of reduced wave power
353 which coincided with this welding phase (Fig 6ii).

354

355 For the morphological evolution of intertidal bars reported here, infilling of the runnel
356 landward of the advancing bar crest took place through slip face progradation.

357 Shallowing of the runnel was accomplished through deposition on its floor of the excess
358 sediment that was not removed by shore-parallel currents in the runnels. Progressive
359 infilling reduced the water discharge through the runnels leading to reduced efficiency.

360 Under these conditions, a positive feedback mechanisms whereby reduced currents in the
361 runnel facilitate more rapid progradation of the slip face, and the ultimate closure of the
362 runnel, is considered to have occurred.

363

364 The observations presented imply that under high wave energy conditions, waves exert
365 the primary influence on bar migration rates whilst tidal influence, although a
366 contributing factor in helping to decelerate or accelerate bar migration patterns, appears

367 to adopt a more subordinate role under the conditions examined in this study. During the
368 first two successive high energy events, both bars C and A display a deceleration of their
369 onshore migration rates and then subsequent to these higher energy events, the bars
370 regain their accelerated onshore migration behaviour. The third high energy wave event,
371 when normalised with tides to give a weighted wave power, actually shows a
372 significantly lower normalised wave power than the previous two events. Bar A during
373 this phase of lower wave forcing still shows onshore migration but at a slower rate.
374 Migration patterns appear to be controlled by the interaction of tidal range and wave
375 action, resulting in enhanced onshore migration. There is also a spatial dimension in that
376 more landward and sheltered bars are less affected by incident wave energy than those in
377 seaward positions.

378

379 The scatter of values (Fig. 7) of migration rate vs. normalised wave power under lower
380 wave conditions in the study area suggests that both wave energy and tidal range play
381 roles that are difficult to separate, but that above a certain threshold ($H_s \cong 1\text{m}$; $P_n: 2000$
382 W/m) wave action becomes dominant, particularly in bar C which is the most exposed
383 bar to incident waves.

384

385 As the bars migrate onshore they reach higher levels in the tidal frame and would
386 therefore be expected to slow down due to less frequent overtopping (Wijnberg and
387 Kroon 2002). This is not apparent in our observations and may be due to enhanced swash
388 run-up overcoming any additional elevation reached by the migrating bars.

389

390 Most previous studies (Wijnberg & Kroon 2002; Masselink et al. 2006) have been in
391 moderate to low wave energy environments. In those settings, tidal water levels can be
392 demonstrated to play an important role in bar migration. In contrast, even though the
393 tidal range is relatively large in our study area (3.8m), wave energy exerts a dominant
394 influence on migration patterns of the seaward (and therefore more exposed) bars. This
395 points to a different, wave-dominated domain of bar behaviour that contrasts with tide-
396 dominance in low wave energy settings.

397

398

6. CONCLUSIONS

399 This study examines the short-term (9-week) behaviour of intertidal bars on a high energy
400 coast using DGPS topographical surveys, detailed nearshore wave modelling combined
401 with local tide levels. Several high-energy wave events were identified during this period.
402 Over the entire study period all bars largely migrated onshore but this behaviour was not
403 regular and was mostly related to energetic wave conditions and intervening lower energy
404 phases. In general, higher energy events resulted in a deceleration of the onshore bar
405 migration rates, whilst in lower wave energy periods, bars accelerated in their onshore
406 migration. This behaviour is reflected most in the northern part of the beach where bars C
407 and A are located. However, bar A being sheltered by the seaward-fronting Bar C, has a
408 more muted behavioural response to this forcing. Bar B is also sheltered by the presence
409 of offshore submerged sand bodies and is close to the inlet channel edge. This results in
410 wave energy reduction at Bar B which is reflected in the relatively low but steady bar
411 migration rates of Bar B over the entire study period.

412 In general, wave forcing is the main driver of changes in bar migration patterns at the
413 site, helping to accelerate (low energy conditions) and decelerate (high energy) the rate of
414 onshore migration. Tidal influence also contributes to bar behaviour at the site but has a
415 more subordinate role compared to wave forcing (evidenced by the normalised wave
416 power data), helping to moderate localised wave energy and maintaining runnel flushing
417 within tidal cycles.

418 This short-term study provides valuable insights into post-storm beach recovery
419 mechanisms along high-energy sandy coasts, particularly when intertidal sand bars are
420 present and are on the process of welding back onto the beachface.

421 **Acknowledgments**

422 Funding from Donegal County council is acknowledged for this work as part of a PhD
423 studentship. Access to high-resolution bathymetric data was provided by the INFOMAR
424 project, a joint seabed mapping project between the Geological Survey of Ireland and the
425 Marine Institute. The use of the Joint Irish Bathymetric Survey dataset was made possible
426 by the Maritime and Coast Guard Agency (UK), the Marine Institute of Ireland, the
427 Northern Ireland Environment Agency (NIEA) and the Geological Surveys of Ireland
428 (GSI) and Northern Ireland (GSNI). The authors would also like to acknowledge the
429 Marine Institute for kindly providing the M4 wave records and Malin Head tide
430 predictions, as well as the UK Met Office for the hindcast wave data. LANDSAT
431 imagery was available from the U.S. Geological Survey Earth Explorer Platform. CL was
432 supported by Fundação para a Ciência e Tecnologia (Grant Reference
433 SFRH/BPD/85335/2912). Two anonymous referees are acknowledged for helping to
434 improve the manuscript.

435

436 **FIGURE CAPTIONS**

437 **Figure 1.** Location of Five Finger Strand within Trawbreaga Bay, Northwest Ireland.

438 Map is based on the ordnance survey map of 1904.

439

440 **Figure 2.** Photo of Five Finger beach site (i), showing profile lines 1 and 3 and cross

441 sections through each at the start of the survey (ii and iii).

442

443 **Figure 3.** Location of the computational grids used for wave modelling simulations, (i)

444 100m resolution grid and (ii) 30 m nested grid.

445

446 **Figure 4.** Sequential profiles of bars A and C showing (i) overall profiles of Bars A and

447 C (ii) Zoomed view of bar C slip face and crest and (iii) zoomed view of Bar A slip face

448 and crest.

449

450 **Figure 5.** Sequential profiles of bar B showing (i) overall profile, and (ii) zoomed view

451 of Bar B slip face and crest

452

453 **Figure 6.** (i) Bar migration rates. Note that descending parts of the graph represent

454 acceleration bar migration rates whilst ascending indicates deceleration of migration

455 rates. Note that most of the migration for all bars was onshore during the study period.

456 (ii) nearshore significant wave heights and normalised wave power. A total of four higher

457 energy events can be observed. Note that the normalised wave power plot can at times

458 show reduced wave energy levels with coincident with lower tidal stages and (iii) tidal
459 elevations during the experiment. Note periods of neap tides are highlighted.

460

461 **Figure 7.** Bar migration rates vs. normalised wave power for (i) Bar A, (ii) Bar B and
462 (iii) Bar C. Note that Bar C displays the best correlation (r^2 value 0.84; P value 0.04 and
463 therefore result is significant at $p < 0.05$) in terms of forcing and response and this is likely
464 due to its exposed location relative to other bar positions (P values not significant at
465 $p < 0.05$ and low r^2 values).

466

467

468

469 **References:**

470

471 AAGARD, T., HUGHES, M., MOLLER-SORENSEN, R. AND ANDERSEN, S., 2006,
472 Hydrodynamics and sediment fluxes across an onshore migrating intertidal bar: Journal
473 of Coastal Research, v. 22, 2, p. 247-259.

474

475 ANTHONY, E.J., LEVOY, F., MONTFORT, O. 2004, Morphodynamics of intertidal
476 bars on a mega tidal beach, Merlimont, Northern France. Marine Geology, 208, 73-100.

477

478 ANTHONY, E.J., LEVOY, F., MONTFORT, O., DEGRYSE-KULKARNI, C. 2005,
479 Short-term intertidal bar mobility on a ridge and runnel beach, Merlimont, Northern
480 France. Earth Surface Processes and Landforms, 30, 81-93.

481

482 AUBREY, D., 1979, Seasonal patterns of onshore/offshore sediment movement. Journal
483 of Geophysical Research, v. 84, p. 6347-6354.

484

485 BOOIJ, N., RIS, R.C., HOLTHUIJSEN, L.H. 1999. A third generation wave model for
486 coastal regions. 1. Model description and validation. Journal of Geophysical Research: v.
487 104 (C4), p. 649-7666.

488

489 BRADBURY A.P., MASON T.E., HOLT M.W., 2004. Comparison of the performance
490 of the Met Office UK-Waters wave model with a network of shallow water moored buoy
491 data. Proceedings of the 8th International Workshop on Wave Hindcasting and
492 Forecasting. WMO Technical Document No. 1319. G1-15p

493 COOPER, J.A.G., MCKENNA, J., JACKSON, D.W.T., O'CONNOR, M., 2007,
494 Mesoscale coastal behavior related to morphological self-adjustment. *Geology*, 35 (1)
495 187-190.
496
497 ELGAR, S., GALLAGHER, E. L. AND GUZA, R. T., 2001, Nearshore sandbar
498 migration: *Journal of Geophysical Research*, v.106, p. 11623-11628.
499
500 GALLAGHER, E.L. ELGAR, S, AND GUZA, R.T., 1998, Observations of sandbar
501 evolution on a natural beach: *Journal of Geophysical Research*, v.103, p. 3203-3215.
502
503 GELFENBAUM, G. AND BROOKS, G.R., 2003, The morphology and migration of
504 transverse bars off the west-central Florida coast: *Marine Geology*, v. 200, p. 273 –289.
505
506 GOLDING B., 1983. A wave prediction system for real-time sea-state forecasting.
507 *Quarterly Journal Royal Meteorological Society*: v. 109, p. 393-416.
508
509 HASSELMANN K., BARNETT T.P., BOWS E., CARLSON H., CARTWRIGHT D.E.,
510 ENKE K., EWING J.A., GIENAPP H., HASSELMANN D.E., KRUSEMAN P.,
511 MEERBURG A., MÜLLER P., OLBERS D.J., RICHTER K., SELL W., WALDEN H.,
512 1973. Measurements of wind–wave growth and swell decay during the Joint North Sea
513 Wave Project (JONSWAP). *Ergänzungsheft zur Deutschen Hydrographischen Zeitschrift*,
514 A8 (12), 1–95.
515

516 HUANG, J., JACKSON, D.W.T. AND COOPER, J.A.G., 2002, Morphological
517 monitoring of a high energy beach system using GPS and total station techniques: Journal
518 of Coastal Research, v. SI 36, p. 390-398.
519

520 JACKSON, D.W.T., COOPER, J.A.G. AND DEL RIO, L., 2005, Geological control of
521 beach morphodynamic state: Marine Geology, v. 216, p. 297–314
522

523 JACKSON, D.W.T., ANFUSO, G. and LYNCH, K. (2007) Swash bar dynamics on a
524 high-energy mesotidal beach. Journal of Coastal Research, SI 50. pp. 738-745.
525

526 JAFFE, B.E. AND RUBIN, D.M., 1996, Using non-linear forecasting to determine the
527 magnitude and phasing of time-varying sediment suspension in the surf zone: Journal of
528 Geophysical Research, v. 101, p. 14283-14296.
529

530 LEVOY, F., ANTHONY, E.J., MONTFORT, O., LARSONNEUR, C., 2000, The
531 morphodynamics of megatidal beaches in Normandy, France: implications for the
532 application of beach environmental parameters. Marine Geology, 171, 39-59.
533

534 LOUREIRO, C., FERREIRA, C., COOPER, J.A.G., 2012. Geologically constrained
535 morphological variability and boundary effects on embayed beaches. Marine Geology, v.
536 329-331, p. 1-15.
537

538 MASSELINK, G., KROON, A. AND DAVIDSON-ARNOTT, R.G.D., 2006,
539 Morphodynamics of intertidal bars in wave-dominated coastal settings: A review:
540 Geomorphology, v. 73, p. 33-49.
541
542 MORRIS, B.D., DAVIDSON, M., HUNTLEY, D., 2001. Measurements of the response
543 of a coastal inlet using video monitoring techniques. Marine Geology, v. 175, p. 251–272.
544
545 O’CONNOR, M., COOPER, J.A.G., JACKSON, D.W.T., 2011. Decadal behaviour of
546 tidal inlet-associated beach systems, Northwest Ireland, in relation to climate forcing:
547 Journal of Sedimentary Research, v. 81, p. 38-51.
548
549 OSBORNE, P. AND GREENWOOD, B., 1993, Sediment suspension under waves and
550 currents: timescales and vertical structure: Sedimentology, v. 40, p. 599-688.
551
552 PACHECO, A., HORTA, J., LOUREIRO, C., FERREIRA, O., 2015. Retrieval of
553 nearshore bathymetry from Landsat 8 images: A tool for coastal monitoring in shallow
554 waters. Remote Sensing of Environment: v. 159, p. 102-116.
555
556 RIS, R.C., HOLTHUIJSEN, L.H., BOOIJ, N., 1999. A third-generation wave model for
557 coastal regions - 2. Verification. Journal of Geophysical Research: v. 104 (C4), p. 7667–
558 7681.
559

560 ROY, P.S., COWELL, P.J., FERLAND, M.A. AND THOM, B.G. 1994, *In*: Carter,
561 R.W.G. & C.D. Woodroffe (eds) Coastal Evolution. Cambridge University Press: p. 121–
562 186.
563
564 RUESSINK, B. G. AND TERWINDT, J. H. J., 2000, The behaviour of nearshore bars on
565 the time scale of years: a conceptual model: Marine Geology, v. 63 (1-4), p. 289-302.
566
567 RUESSINK, B. G., BELL, P. S., VAN ENCKEVORT, I. M. J. AND AARNINKHOF, S.
568 G. J., 2002, Nearshore bar crest location quantified from time-averaged X-band radar
569 images: Coastal Engineering, v. 5 (1), p. 19-32.
570
571 SALMON, J., HOLTHUIJSEN, L., 2011. Re-scaling the Battjes-Janssen model for
572 depth-induced wave breaking. Proceedings of the 12th International Workshop on Wave
573 Hindcasting and Forecasting. WMO/JCOMM Technical Report No. 67. 13-6p.
574
575 STOKES, C., DAVIDSON, M., RUSSEL, P., 2015. Observation and prediction of three-
576 dimensional morphology at a high-energy macrotidal beach. Geomorphology, v. 243, p.
577 1-13.
578
579 THORNTON, E., HUMISTON, R. AND BIRKEMEIER, W., 1996. Bar-trough
580 generation on a natural beach: Journal of Geophysical Research, v.101, p. 12097-12110.
581

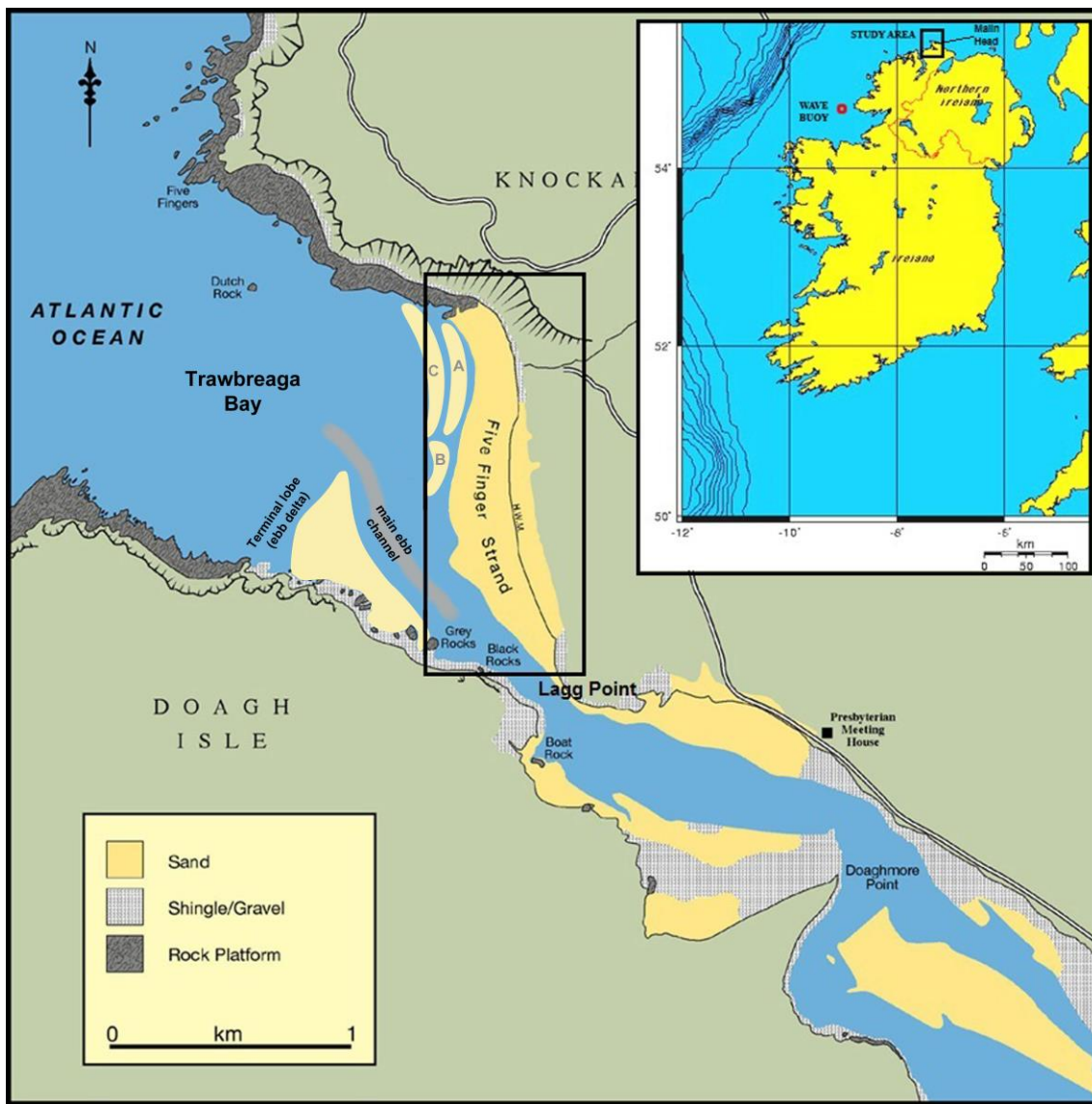
582 WIJNBERG, K. AND KROON, A., 2002, Barred beaches: Geomorphology, v. 48, p.103-
583 120.

584

585 WRIGHT, L.D. AND SHORT, A.D., 1984, Morphodynamic variability of surf zones and
586 beaches: a synthesis: Marine Geology, v. 56, p. 93-118.

587

588 [Figure1](#)



589

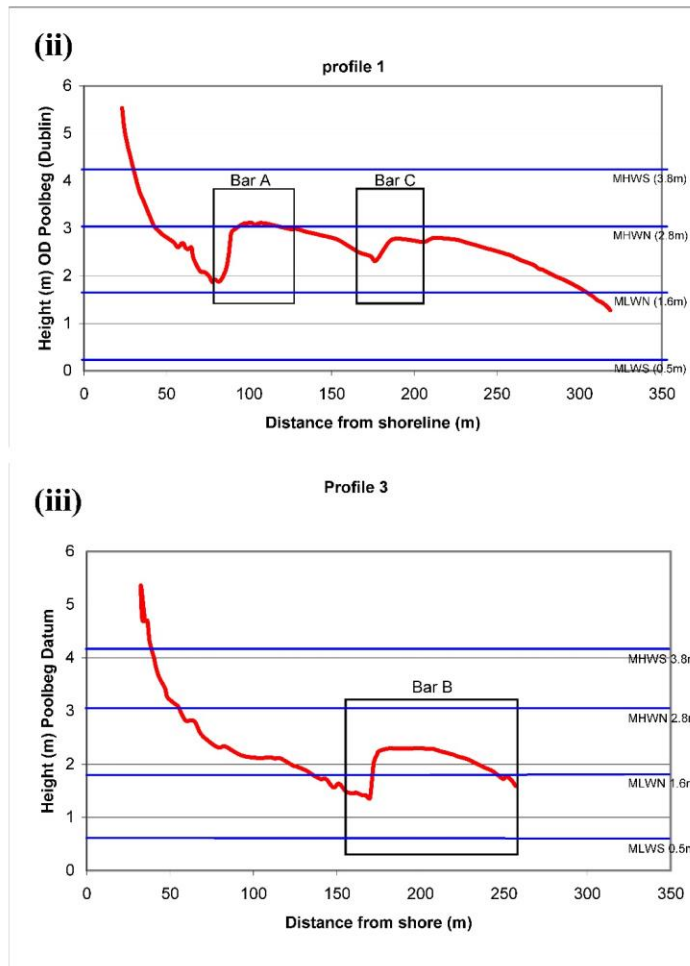
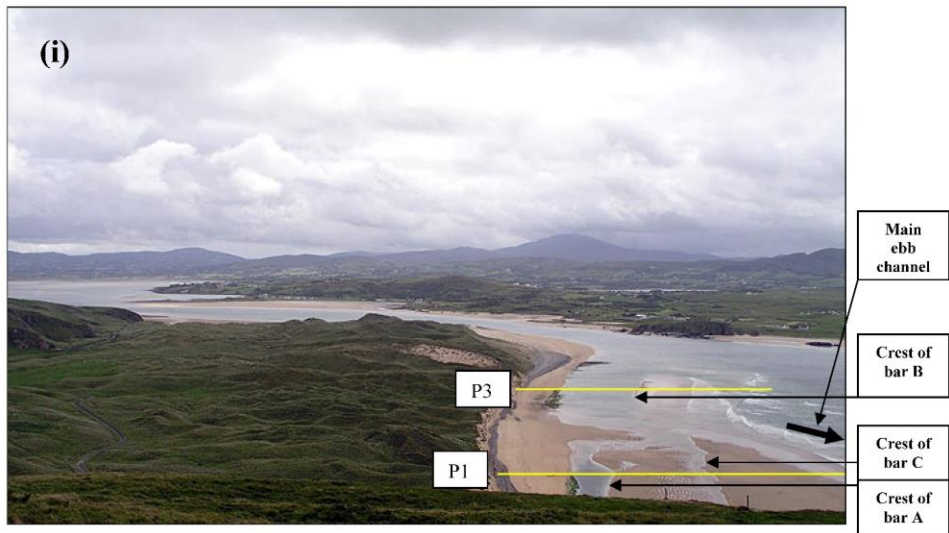
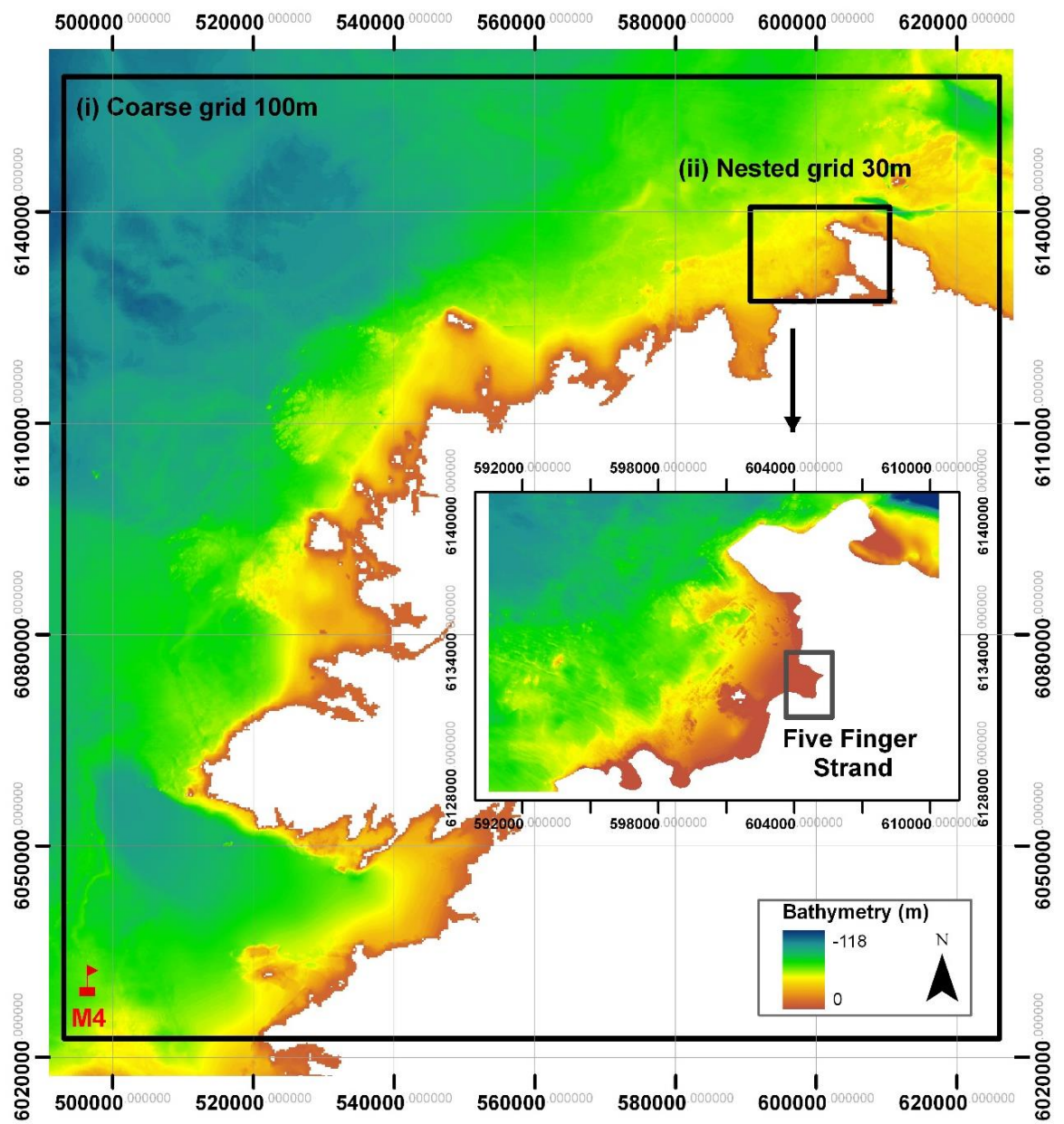


FIGURE 2



591
592

[Fig. 3](#)

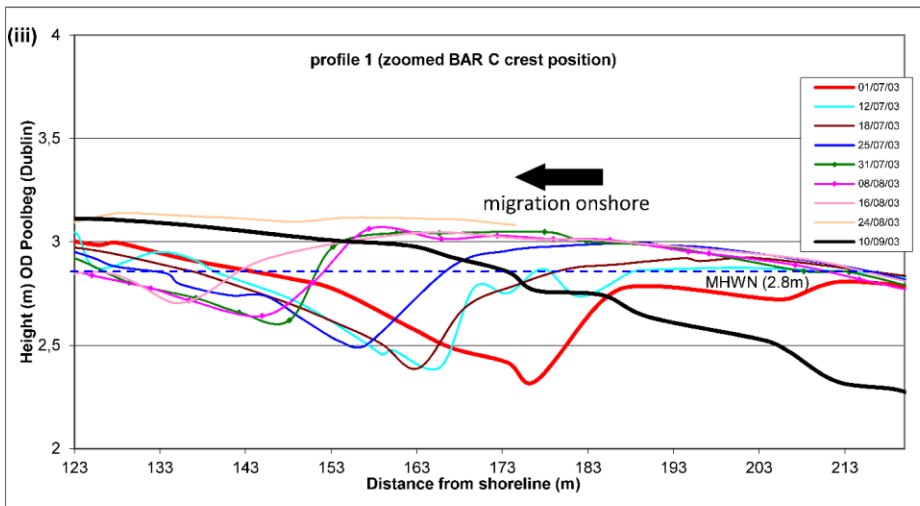
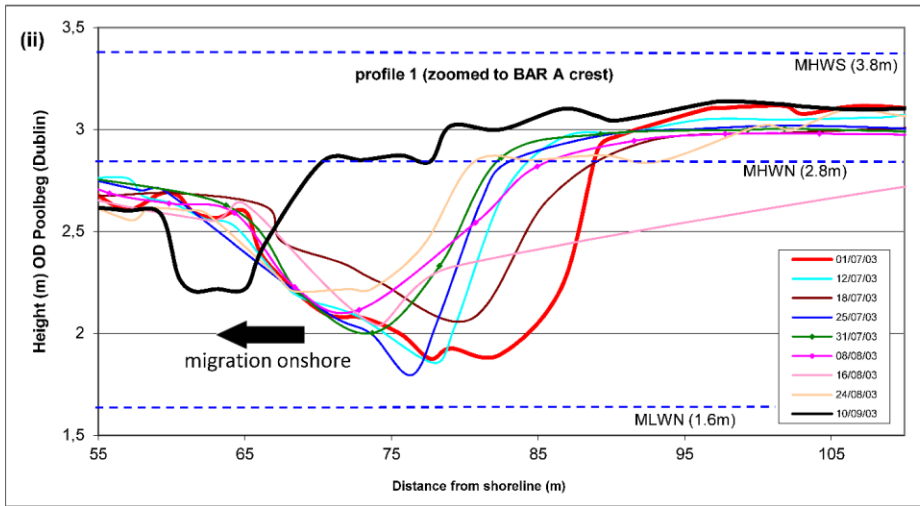
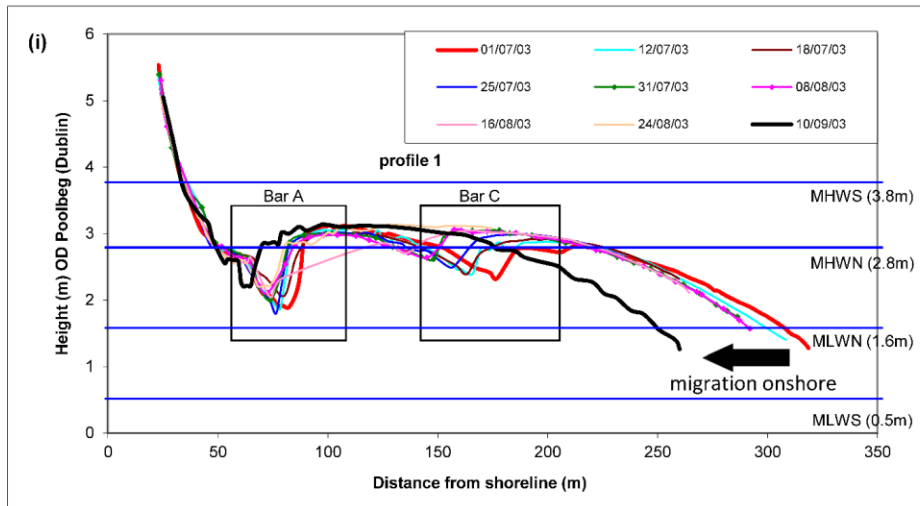


FIG.4

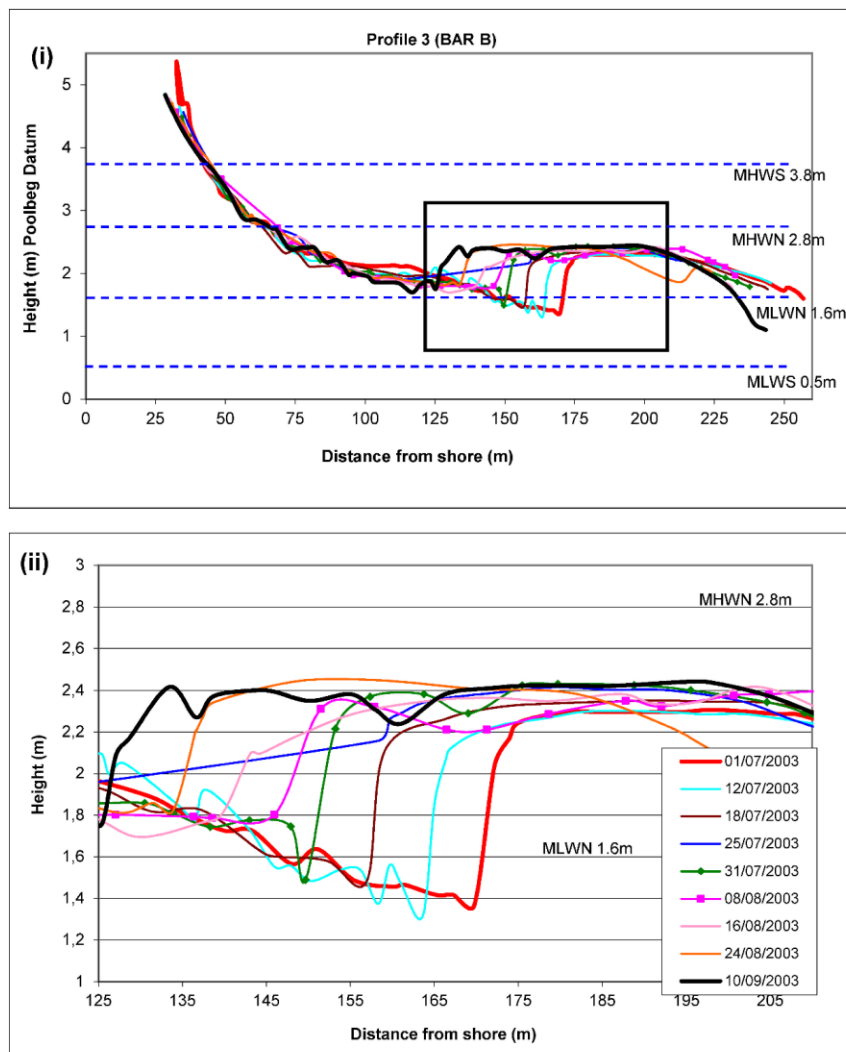


FIGURE 5

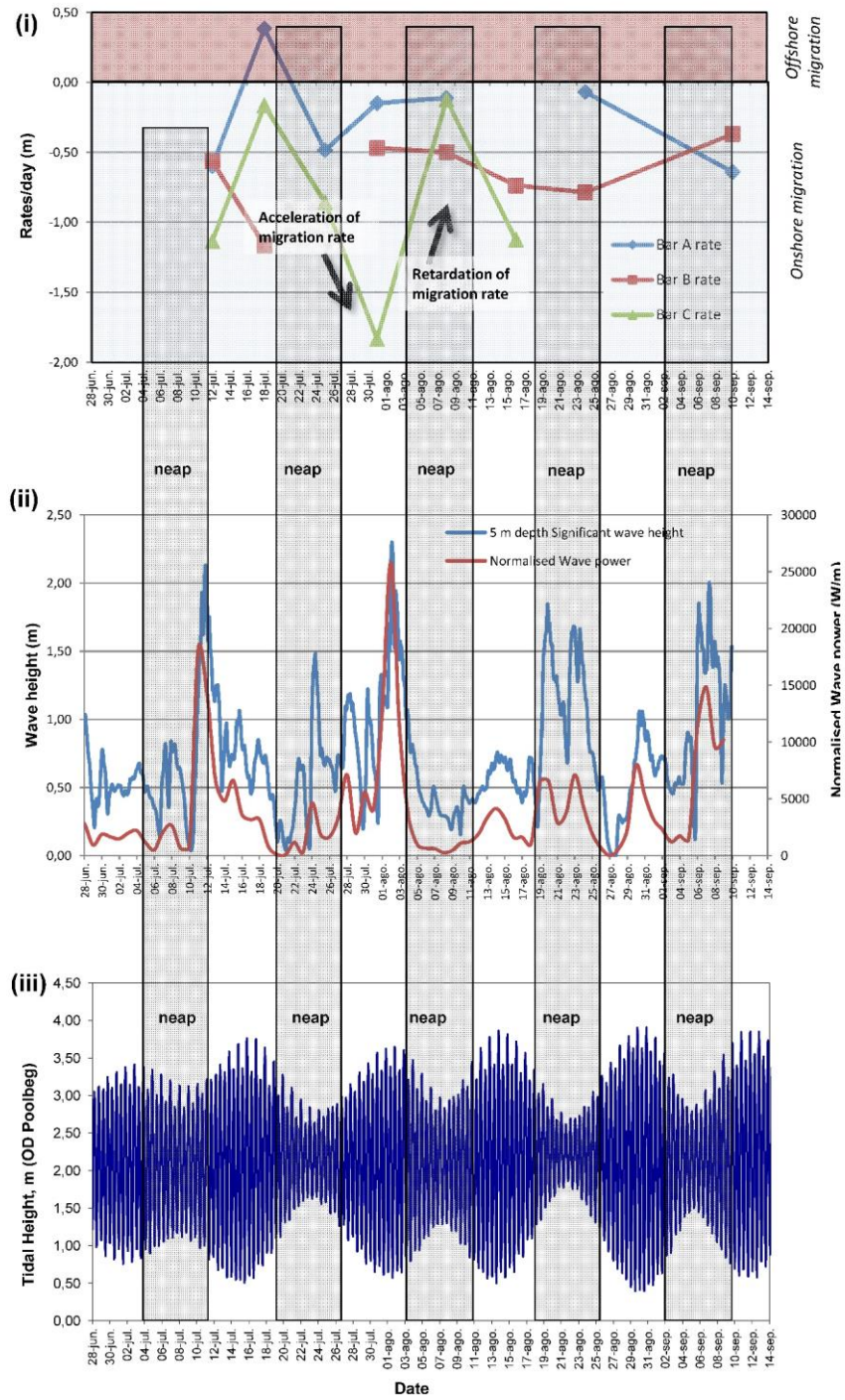


FIGURE 6

